RSC Advances

PAPER

Cite this: *RSC Adv.*, 2022, **12**, 285

Outstanding flame retardancy for poly(vinyl alcohol) achieved using a resveratrol/tannic acid complex

Yuan Lin,[ab] Jialian Chen[a] and Hongzhou Li *[ab]

Received 1st November 2021
Accepted 13th December 2021

DOI: 10.1039/d1ra08000h

rsc.li/rsc-advances

Resveratrol/tannic acid-poly(vinyl alcohol) (RETA-PVA) blends have been prepared by compression molding using poly(vinyl alcohol), tannic acid and resveratrol as raw materials. The effects of different resveratrol/tannic acid ratios on the flammability of RETA-PVA blends have been studied. The flammability of the RETA-PVA blends was assessed using cone calorimetry, thermogravimetric analysis (TGA) and differential scanning calorimetry (DSC). Results indicate that RETA-PVA molecules occur through hydrogen bonding and RETA-PVA blends are amorphous. The glass transition temperature for RETA-PVA-2 is the highest among all blends and the peak of heat release rate and smoke production rate for RETA-PVA is 38.4% and 43.9% lower than that for PVA, respectively. With the addition of resveratrol, the residual amount of RETA-PVA after complete combustion is greatly increased, to 30 times that for PVA, indicating that RETA-PVA blends display excellent flame retardant properties.

1 Introduction

Traditional halogen-containing flame retardants, such as polybrominated biphenyls and polychlorinated biphenyls, are largely no longer used due to toxicity, carcinogenicity, bioaccumulation and other factors that can lead to irreparable harm to human health and the natural environment.[1,2] In recent years, phosphorus–nitrogen flame retardant systems have been widely used as major alternatives to halogenated flame retardants because of great effectiveness and low toxicity. However, the release of organophosphorus flame retardants may lead to eutrophication in waterways. In addition, phosphorus-containing flame retardants containing *N*-methylol groups may release formaldehyde upon decomposition.[3] Moreover, although phosphorus flame retardants display high flame retardancy, they may also reduce the mechanical properties of a polymer matrix into which they are incorporated.[4,5] Therefore, in order to meet the needs of environmental safety and sustainable development, there is an urgent need to develop environmentally-friendly flame retardants. Cellulose/montmorillonite nanocomposite biobased plastics have been synthesized, which can be used in the fields of gas resistance, flame retardancy and packaging.[6] The use of abundant renewable, safe and non-toxic compounds and their derivatives from nature as components of flame retardant materials has become a major focus for polymer flame retardancy.[1–3,7,8] Effective biobased organophosphorus flame retardants based on a variety natural source have been developed.[9]

Poly(vinyl alcohol) (PVA) is the only biodegradable polymer that contains exclusively carbon atoms in the mainchain.[10] PVA has been widely used in various fields, such as paper coating, adhesive formulation and glue production, *etc.*, because of the properties of biocompatibility, hydrophilicity, excellent film-forming properties, cross-linking potential and crystallization propensity.[11] However, PVA is inherent flammable and upon combustion releases large amounts of heat and smoke. Therefore, means to generate flame retardant PVA has become more and more important in recent years.

Tannic acid (TA) is a natural polyphenol which may be extracted from plants. It has a carbon content of up to 53.6%.[12] Its unique phenolic hydroxyl structure endows it with a series of chemical properties, including the ability to scavenge radicals, antibacterial properties, high adhesion, good char forming capability and the ability to form a complex layer with metal ions on a polymer matrix, *etc.*[8,13,14] TA displays excellent promotion of char-formation and oxygen radical scavenging during the combustion process.[15,16] Therefore, TA can be used as an environmentally-friendly flame retardant. A two-dimensional nanosheet formed of TA and MoS_2 can be used to improve the mechanical properties and flame retardancy of polyacrylonitrile fibers. Grafting a 2% weight fraction of two-dimensional nanoflake on the surface of polyacrylonitrile fiber provided a 70.4% increase in tensile strength and a 54.2% increase in elongation at break. The peak heat release rate, the total heat release, and the peak smoke production rate and the carbon monoxide production decreased by 38.1%, 29.6%,

[a]*College of Environmental Science and Engineering, Fujian Normal University, Fuzhou, 350007, China*

[b]*Engineering Research Center of Polymer Resources Green Recycling of Ministry of Education, Fuzhou, 350007, China. E-mail: lihongzhou@fjnu.edu.cn*

34.0% and 34.9%, respectively.[17] However, the melting point of TA is only 218 °C and its heat stability is poor.

Resveratrol (RE) is a natural trihydroxy stilbene compound. RE and its derivatives are mainly found in grapes, peanuts, and knotweed.[18–23] Because of its antioxidant, anti-inflammatory, anti-cancer and cardiovascular protection effects, it is widely used in medicine, food and other fields. As a derivative of stilbene, due to its functional phenolic hydroxyl group and rigid conjugated structure, it has also been extensively utilized in the field of flame retardancy.[24,25] RE-based tri-functional benzoxazine resin has been synthesized, its thermal properties established using thermogravimetric analysis (TGA) and micro-scale combustion calorimetry (MCC).[25] The glass transition temperature for the RE-based resin is higher than 350 °C, the initial degradation temperature is 465 °C, the corresponding mass loss is only 10%, and the carbon residue from combustion may be as high as 74% of the initial mass at 800 °C. The resin also exhibits extremely low heat release capacity (30.7 J g^{-1} K^{-1}) and total heat release value (6.0 kJ g^{-1}) during combustion.[25] A RE-based epoxy resin has been synthesized and cured with methyl hexahydrophthalic anhydride.[26] The glass transition temperature for the RE-based epoxy resin is 211.1 °C, and the tensile strength, tensile modulus and tensile strain are 73.5 ± 3.9 MPa, 3.0 ± 0.1 GPa and 3.4 ± 0.3%, respectively. The decomposition residue at 800 °C is twice than that for petroleum-based epoxy resin. Therefore, RE can be considered as a natural material with high flame retardant potential.[26]

Using the characteristics of TA with multiple hydrogen bond sites treatment with RE was utilized to form a hydrogen-bonded complex (RETA). The RETA was used to form a blend with PVA, RETA-PVA. The molecular structure of RETA-PVA was assessed using Fourier transform infrared spectroscopy. Due to the large number of hydroxyl functional groups on the mainchain of PVA, RETA may form hydrogen bonds with PVA fully and effectively. This affords weak cross-linking to form a network structure.[27–29] The flammability properties of RETA were evaluated using cone calorimetry and thermogravimetric analysis. RETA has not previously been identified as a biobased flame retardant. The presence of RETA in the polymer matrix strong reduces the flammability of PVA. The polyhydroxy structure of TA and RE promotes excellent char formation during the thermal degradation of PVA.

2 Materials and methods

2.1 Materials

Polyvinyl alcohol (PVA, type 1788), resveratrol (RE, 99%) and tannic acid (TA, analytically pure) were purchased from Shanghai Macklin Biochemical Technology Co., Ltd.

2.2 Preparation of RETA-PVA blends

TA was added to a beaker filled with ultrapure water and dispersed by ultrasound at 60 °C for 15 minutes to dissolve into a TA solution. RE was added into the TA solution and stirred at 60 °C for 15 minutes to form a RETA solution. PVA (5 wt%) was added into a 500 ml beaker filled with ultrapure water and stirred it in an oil bath at 85 °C for 30 minutes to dissolve into a PVA solution. The RETA solution was slowly poured into the PVA solution along the wall of the cup and stirred for 30 minutes to form a RETA-PVA precipitate.

The obtained RETA-PVA precipitate was placed in a mold after drying at reduced pressure and the temperature of the upper and lower plates of a plate vulcanizing machine is set to 100 °C. The sample was formed in hot pressing for 10 minutes and cold pressing for 5 minutes under the pressure of 10 MPa. Then, the sample was placed in an oven at 60 °C and cooled to constant weight to obtain RETA-PVA blends. The formula of RETA-PVA is shown in Table 1. The preparation route diagram of RETA-PVA is shown in Fig. 1. Fig. 2 shows the synthetic route of the RETA-PVA.

2.3 Characterization

2.3.1 FTIR. Fourier transform infrared spectroscopy (FTIR) was performed on a Thermo Fisher's NICOLET IS10 Fourier transform infrared spectrometer in a wave-number ranging from 4000 to 400 cm^{-1}.

2.3.2 TGA. The TGA analysis of PVA/TA-PVA/RE-PVA/RETA-PVA was carried out using a SDT Q600 thermogravimetric analyzer. The sample (5–10 mg) was heated from 30 °C to 600 °C at a heating rate of 10 °C min^{-1} in a N_2 atmosphere.

2.3.3 DSC. The DSC analysis of PVA/TA-PVA/RE-PVA/RETA-PVA was performed on a Q20 Differential Scanning Calorimeter. The sample (5–10 mg) was heated from 0 °C to 250 °C at a heating rate of 10 °C min^{-1} in a N_2 atmosphere.

2.3.4 Limit oxygen index (LOI) and vertical combustion test. LOI value of samples was obtained using a JF-3 oxygen index instrument. UL-94 rating of the samples was performed on a CZF-3 horizontal vertical combustion tester.

2.3.5 Cone calorimetry test. The cone calorimetry test was carried out using a FTT iCone classic cone calorimeter. The sample (100 mm × 100 mm × 4 mm) was tested under N_2 and standard gas (CO, CO_2, O_2) atmospheres at a heat radiation flow rate of 35 kW m^{-2} and a cone temperature of 750 °C according to the test standard ISO 5660-1.

2.3.6 Analysis of the microscopic morphology of carbon residue. The carbon residue after cone test was observed under Hitachi's Regulus 8100 scanning electron microscope. The surface of the sample was sprayed with gold and it was observed under 5 kV acceleration voltage.

2.3.7 Mechanical property test. Flexural test was carried out using a CMT-4104 universal testing machine. Impact test was carried out using a ZBC-500 simple-supported beam impact testing machine.

Table 1 Formula of RETA-PVA

Sample	PVA (g)	TA (g)	RE (g)
PVA	5	—	—
TA-PVA	5	4.2	—
RE-PVA	5	—	4.2
RETA-PVA-1	5	3.36	0.84
RETA-PVA-2	5	2.94	1.26
RETA-PVA-3	5	2.52	1.68
RETA-PVA-4	5	2.1	2.1

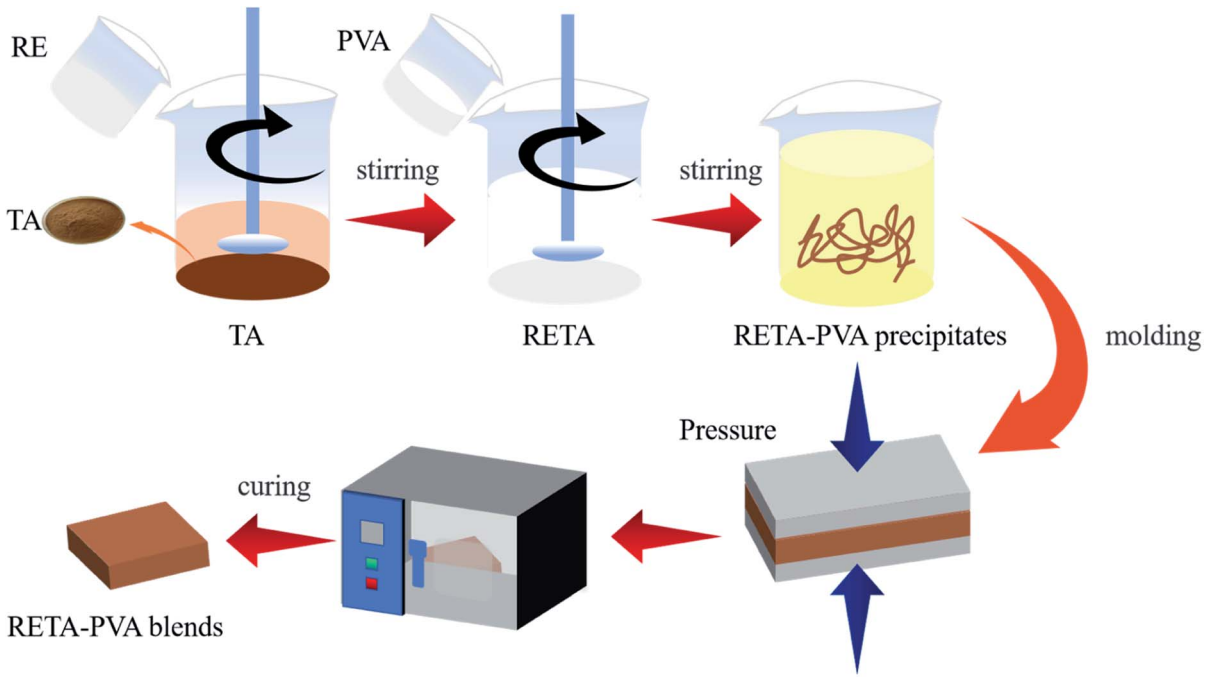

Fig. 1 Preparation route diagram of RETA-PVA.

3 Results and discussion

3.1 Fourier transform infrared spectroscopy

In order to determine the hydrogen bond between RETA and PVA molecules, the Fourier transform infrared spectra of TA/RE/RETA/PVA/TA-PVA/RE-PVA/RETA-PVA were performed on the Thermo Fisher's FTIR. As shown in Fig. 3(a), obvious absorption peaks of TA and RE were observed in the spectra of RETA, indicating that RE and TA were successfully combined. The absorption peaks at 1710 cm^{-1} and 1612 cm^{-1} are the tensile vibration peak of C=O and C=C, respectively. A strong absorption peak appears at 3262 cm^{-1}, 3396 cm^{-1} and 3284 cm^{-1}, which are the stretching vibration peak of the hydroxyl group (–OH), and peak width is formed by the association of multiple phenolic hydroxyl groups. There were slightly differences in the FTIR peaks of RETA-PVA due to the different ratio of RE/TA. It can be seen from the Fig. 3(b) that the intensity of the tensile vibration peak of hydroxyl increases with the increase of RE ratio. The stretching vibration peak of hydroxyl (–OH) at 3445 cm^{-1} in PVA shifted to higher wavenumber with the increase of RE content, for example, a 4 cm^{-1} upshift to 3449 cm^{-1} for RETA-PVA-1, 3 cm^{-1} upshift to 3348 cm^{-1} for RETA-PVA-2 and RETA-PVA-3, 2 cm^{-1} upshift to 3347 cm^{-1} for RETA-PVA-4. The red shift phenomenon demonstrates the existence of intermolecular hydrogen bond in RETA-PVA.

3.2 Thermal stability of RETA-PVA blends

3.2.1 Thermogravimetric analysis of RETA-PVA blends. The thermal stability of PVA/RE-PVA/TA-PVA/RETA-PVA was carried out on a thermogravimetric analyzer. The thermogravimetric data of PVA/RE-PVA/TA-PVA/RETA-PVA is shown in Table 2. The TG and DTG curves of the PVA/RE-PVA/TA-PVA/RETA-PVA samples are shown in Fig. 4. It can be seen from the figure that the TG curves of TA-PVA and RETA-PVA exhibit obvious double degradation peaks. Before 100 °C, the mass loss of TA-PVA and RETA-PVA is mainly the volatilization of water in the blends, thus forming the first degradation peak. TA-PVA decomposes first, and the temperature for RETA-PVA and RE-PVA at mass loss of 10 wt% is higher than that for TA-PVA, indicating that the addition of RE can delay the initial decomposition of the matrix. It may be due to the decomposition of RE can promote the matrix to form carbon during decomposition, then the formation of carbon layer effectively protects the matrix, and RE plays its condensed phase flame retardant role. After 350 °C, the residual amount of RETA-PVA sample is always greater than that of the PVA sample. The residual amount of RETA-PVA-1 sample reached 25% at 600 °C, which is 316.7% higher than that of PVA, indicating that the addition of RETA can promote the carbon formation of PVA. The residual mass content of RE-PVA at 600 °C is as high as 39%.

It can be seen from the DTG curve that the temperature corresponding to the maximum decomposition rate of RETA-PVA was slightly decreased compared with that of the PVA sample. The maximum weight loss peak of RETA-PVA is higher than that of TA-PVA, which indicates that compared with TA-PVA, the maximum decomposition rate of RETA-PVA increased. It can be considered that the faster the RETA-PVA decomposes, the higher its charring efficiency,[30] which may be the reason why the carbon residue of RETA-PVA is always greater than that of TA-PVA.

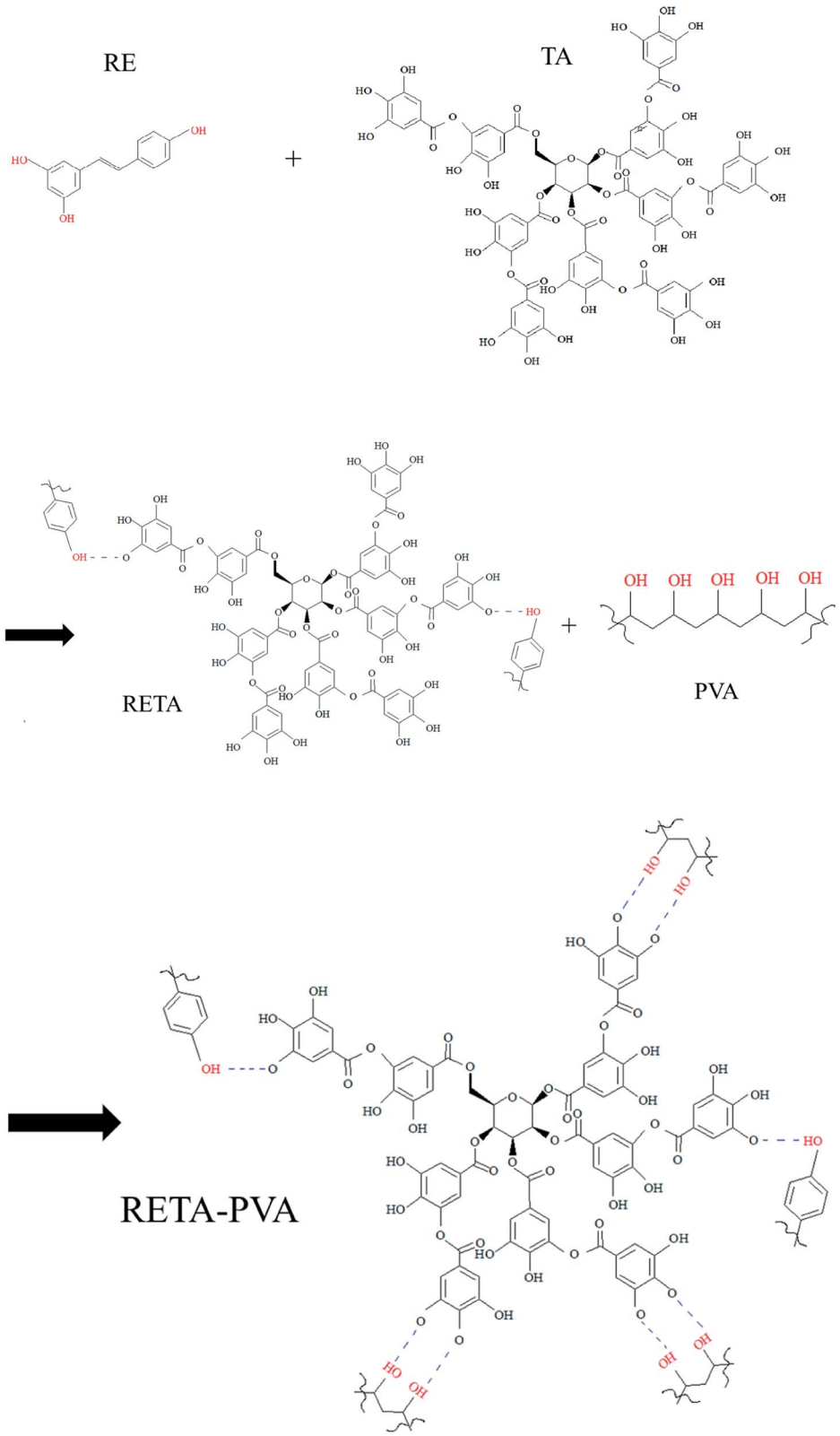

Fig. 2 Synthetic route of RETA-PVA.

TG curve and DTG curve indicate that the maximum decomposition rate of RETA-PVA would be decreased with the addition of RETA, but RETA can slightly promote the decomposition of the PVA matrix earlier because the decomposition temperature corresponding to the maximum decomposition rate is also decreased. During the combustion process,

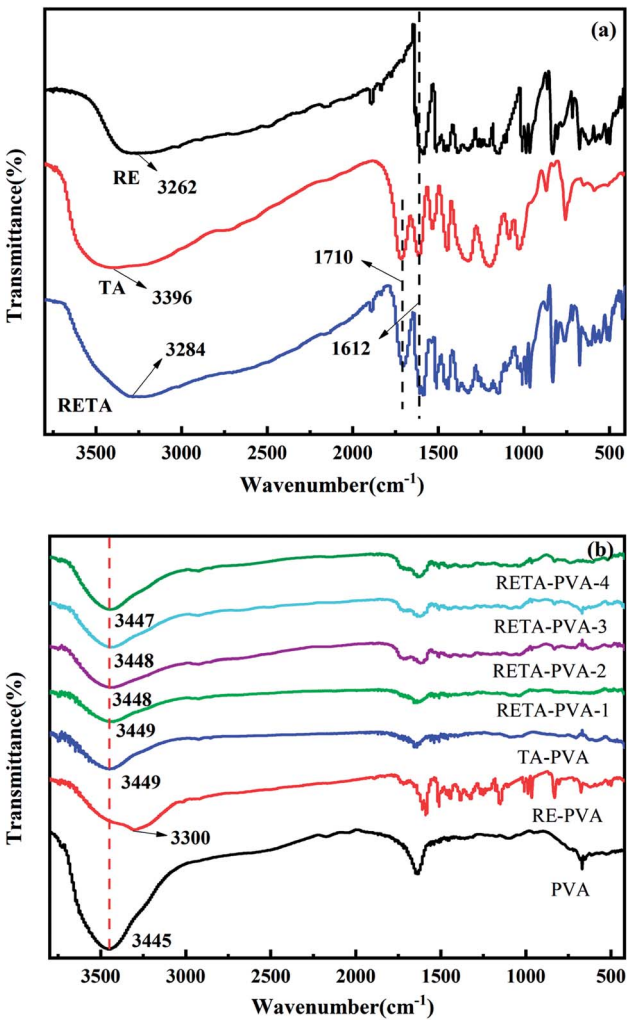

Fig. 3 Fourier transform infrared spectrum: (a) RE/TA/RETA; (b) PVA/RE-PVA/TA-PVA/RETA-PVA blends.

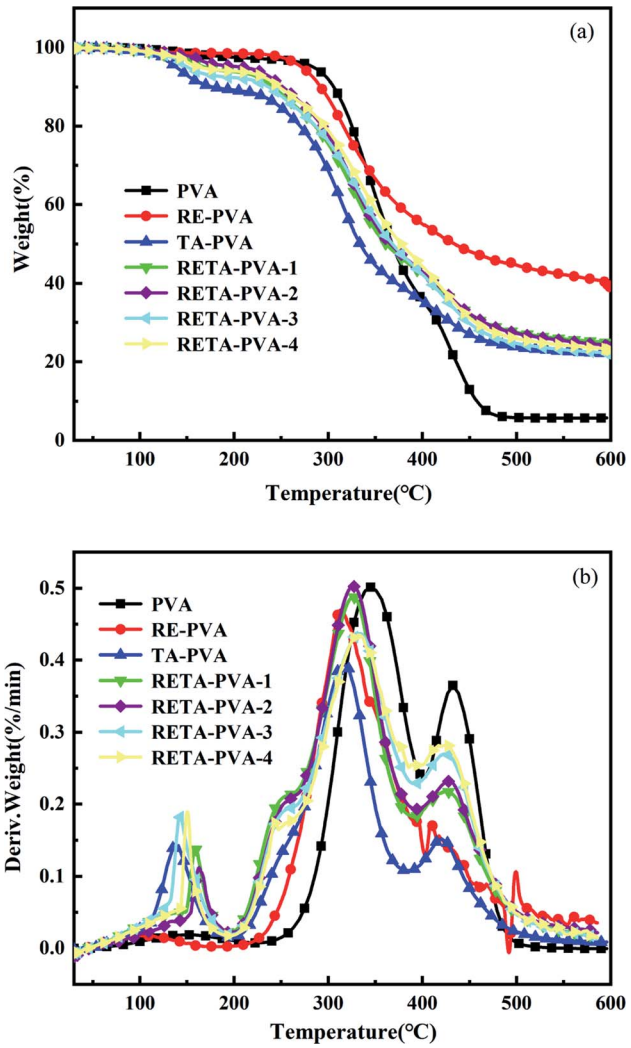

Fig. 4 TG (a) and DTG (b) curves of PVA/RE-PVA/TA-PVA/RETA-PVA.

the residual amount of RETA-PVA is more than that of the PVA at high temperature. It means that RETA-PVA has relatively better thermal stability.

3.2.2 Differential scanning calorimetry analysis of RETA-PVA blends. The thermal transition properties of PVA/TA-PVA/RE-PVA and RETA-PVA containing different ratios of RE and TA were obtained on the Q20 DSC. The DSC curves of heating and cooling of PVA/TA-PVA/RE-PVA/RETA-PVA are shown in Fig. 5(a–g). The glass transition temperature of PVA is 68.8 °C, and the PVA curve displays obvious melting and crystallization peaks, indicating that PVA is a crystalline substance. The DSC curve of TA-PVA shows that the glass transition temperature of TA-PVA is 40.5 °C. However, there is no crystallization peak in the TA-PVA curve and only a degradation peak appears at

Table 2 Thermogravimetric data of PVA/RE-PVA/TA-PVA/RETA-PVA

Sample	$T_{10\ wt\%}$ (°C)	Maximum thermal weight loss temperature (°C)	Char residue at 600 °C (wt%)
PVA	305	345	6
TA-PVA	176	316	22
RE-PVA	292	313	39
RETA-PVA-1	242	327	25
RETA-PVA-2	251	326	24
RETA-PVA-3	236	333	22
RETA-PVA-4	247	332	23

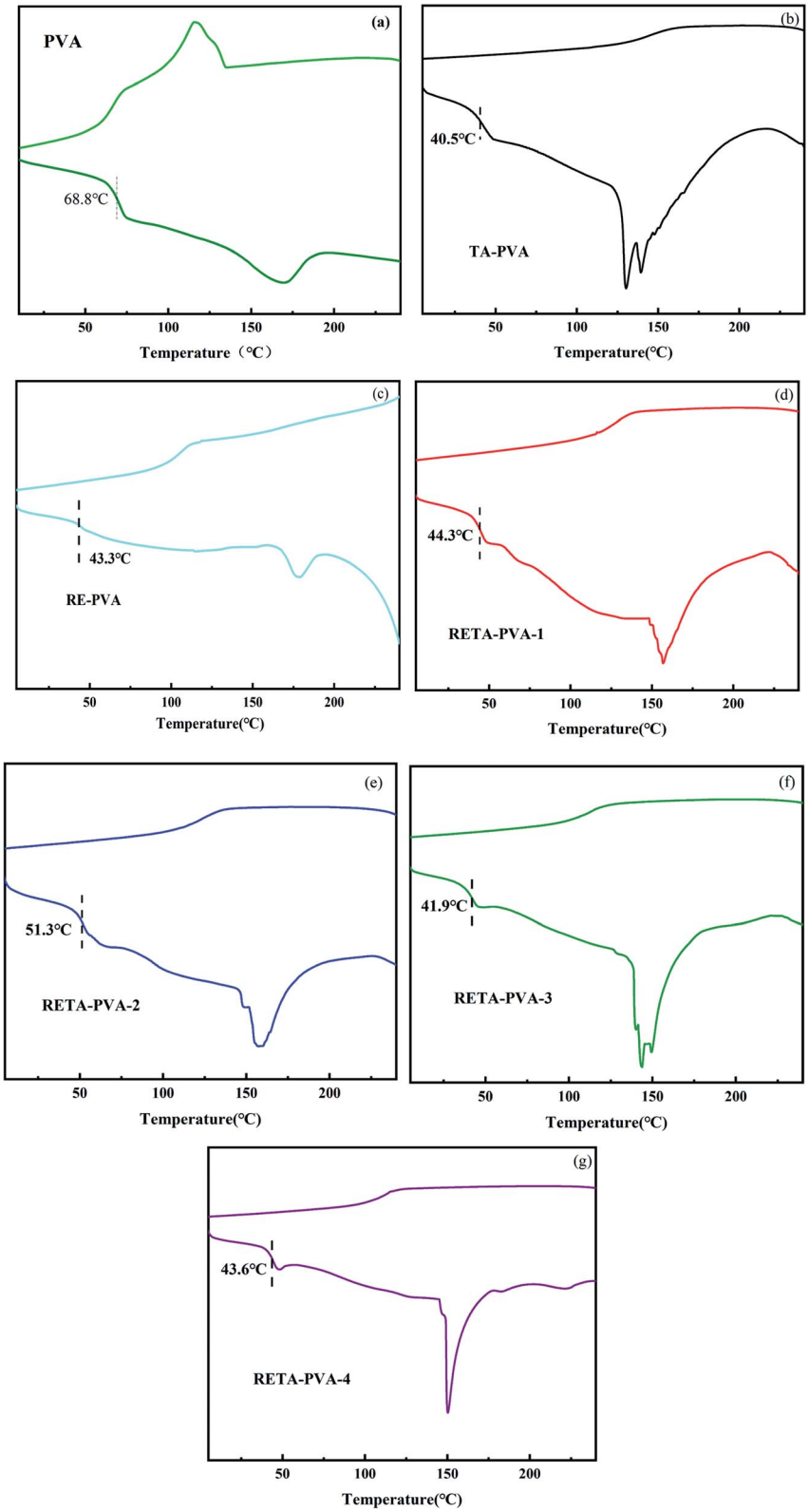

Fig. 5 DSC curves of samples during heating and cooling: (a) PVA, (b) TA-PVA, (c) RE-PVA, (d) RETA-PVA-1, (e) RETA-PVA-2, (f) RETA-PVA-3, (g) RETA-PVA-4.

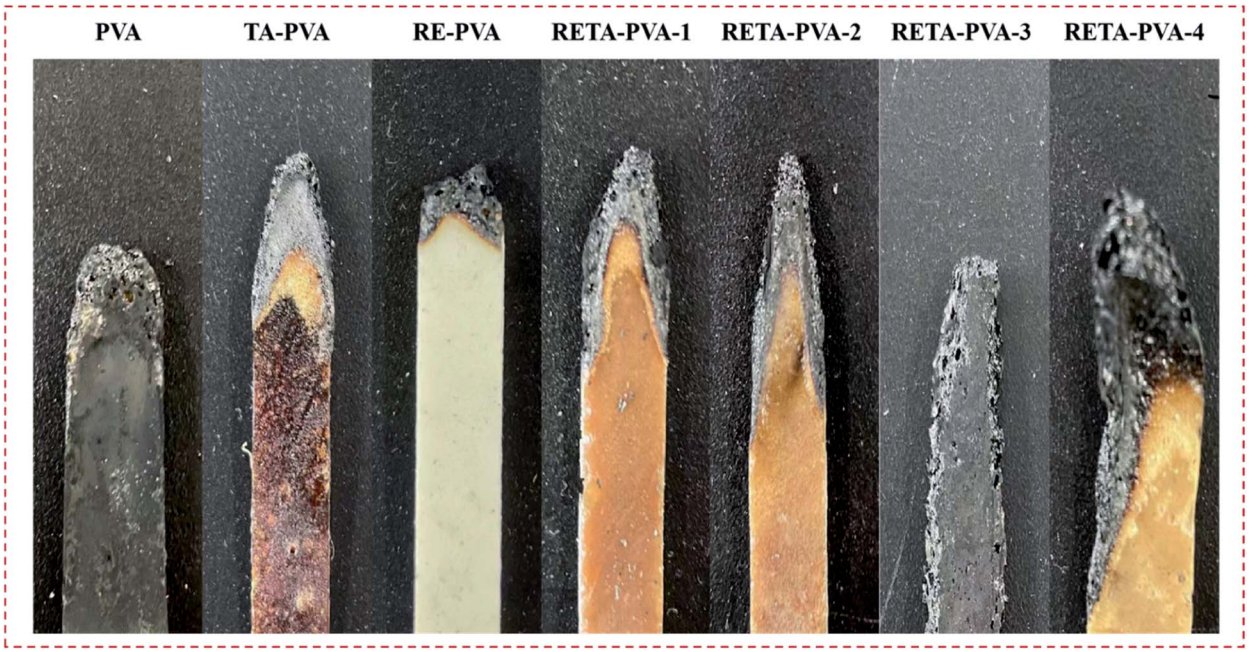

Fig. 6 Digital photos after LOI test of PVA/TA-PVA/RE-PVA/RETA-PVA.

Table 3 LOI and UL-94 data of PVA/RE-PVA/TA-PVA/RETA-PVA

Samples	LOI (%)	UL-94
PVA	19	NR
TA-PVA	31.2	NR
RE-PVA	24.8	NR
RETA-PVA-1	31.2	NR
RETA-PVA-2	31.4	NR
RETA-PVA-3	31.6	NR
RETA-PVA-4	31.8	NR

130 °C, indicating that TA-PVA is an amorphous substance. As shown in the Fig. 5(c–g), it can be found that RE-PVA and RETA-PVA have also no crystallization peak. Therefore, RE-PVA and RETA-PVA are also amorphous substances. The degradation temperature for RETA-PVA is higher than that for TA-PVA, and RETA-PVA also exhibits a higher glass transition temperature than TA-PVA. The glass transition temperature of RETA-PVA was increased due to the restriction of the movement of polymer molecular segments with the addition of RETA, and the increase of the intermolecular hydrogen bond density of RETA-PVA leads to the restriction of chain segment motion, resulting in higher glass transition temperature of RETA-PVA. The glass transition temperature of RETA-PVA-2 is the highest among all blends. It may be due to RETA-PVA molecules reached the most stable mixing state, and the strongest hydrogen bonding appeared at RE : TA = 3 : 7.[27]

3.3 Flame retardancy of RETA-PVA blends

Limiting oxygen index test is a means to characterize the combustion performance of materials. The digital photos after LOI test of PVA/TA-PVA/RE-PVA/RETA-PVA are shown in Fig. 6. The LOI value and UL-94 rating of PVA/TA-PVA/RE-PVA/RETA-PVA are shown in Table 3. The LOI value of pure PVA is 19%, which is extremely combustible.[31] PVA burns very fast and produces a lot of smoke during the LOI test. With the addition of TA, RE and RETA, the LOI value of TA-PVA/RE-PVA/RETA-PVA increases. The LOI value of RE-PVA is 24.8%, which is higher than that of PVA, but it still belongs to the range of combustible materials. The LOI value of TA-PVA and RETA-PVA exceeds 30%, indicating that the existence of TA and RETA can effectively increase the LOI value and improve the flame retardant properties of the material. During the vertical combustion test, samples burned out once they were ignited, and it displayed no rating for all samples.

The combustion performance of polymer materials in a real fire can be evaluated by cone calorimetry test. Therefore, the cone calorimetry method was used to test the flammability of PVA/RE-PVA/TA-PVA and RETA-PVA blends with different ratios of RE/TA. Fig. 7 shows the HRR (heat release rate), THR (total heat release), SPR (smoke production rate) and mass retention curves of PVA/RE-PVA/TA-PVA/RETA-PVA. Table 4 lists the relevant cone calorimetric test data.

The HRR and THR curves of PVA/RE-PVA/TA-PVA/RETA-PVA are shown in Fig. 7(a) and (b). The peak of the heat release rate curve of PVA is sharp and the peak heat release rate reaches 634.9 kW m^{-2}, indicating that PVA releases a lot of heat during combustion. With the addition of TA/RE/RETA, the peak-HRR of TA-PVA/RE-PVA/RETA-PVA samples shows a significant drop, and the peak-HRR for TA-PVA/RE-PVA/RETA-PVA-3 is 488.2, 273.9 and 391.1 kW m^{-2}, which is 23.1%, 56.9% and 38.4% lower than that for PVA, respectively. Moreover, the obvious bimodal phenomenon can be observed in the HRR curve of the RETA-PVA, indicating that the carbon layer formed

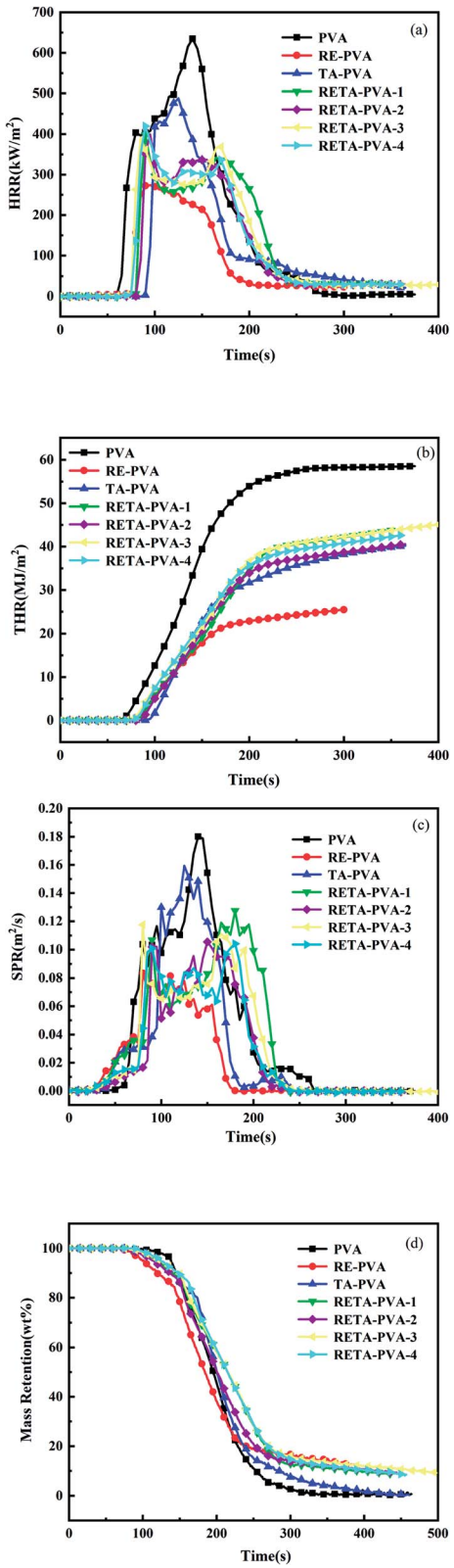

Fig. 7 Cone calorimetric curves of PVA/RE-PVA/TA-PVA/RETA-PVA: (a) HRR, (b) THR, (c) SPR, (d) mass retention.

during the combustion process of the sample can play a physical barrier effect, and effectively protects the PVA matrix. As the sample was further burned, the released heat broke through the carbon layer formed at the beginning of the combustion, resulting in an obvious bimodal phenomenon in the HRR curve. The incombustible gas produced by the decomposition of RE can dilute the concentration of the flammable gas to reduce the heat release rate. At the same time, carbon layer plays the role of condensed phase flame retardancy. The total heat release of RETA-PVA had decreased with the addition of RETA, which can be observed from the THR curve. The total heat release of RETA-PVA-3 is 45.2 MJ m^{-2}, which is the highest among all blends. The increase of THR have certain disadvantages to the security of actual fires. The reason for the increase in total heat release may be caused by the continuous burning of residual char. The TTI (time to ignition) of RETA-PVA increases compared to PVA with the addition of RETA, as shown in Table 4. It means that the addition of RETA has certain beneficial for flame retardancy.

The SPR curves of PVA/RE-PVA/TA-PVA/RETA-PVA are shown in Fig. 7(c). SPR is a particularly important characterization for the flame retardant properties of materials because the burning process of materials may release a large amount of toxic and harmful fumes, which are fatal to human health. Therefore, it is necessary to reduce the SPR of materials as much as possible to rescue people in actual fires. It can be seen from Table 4 that the peak smoke production rate for RETA-PVA-2 is 0.101 m^2 s^{-1}, which is 43.9% lower than that for PVA. It can also be seen from the SPR curve that the SPR peak for RETA-PVA is significantly lower than that for PVA, and the obvious bimodal phenomenon is observed, indicating that the addition of RETA has an inhibitory effect on the rate of smoke production. It may ascribe to the expanded carbon layer formed during the combustion of RETA-PVA, which can play a good barrier and protection effect and reduce the production of smoke particles during combustion.

The mass retention curves of PVA/RE-PVA/TA-PVA/RETA-PVA are shown in Fig. 7(d). With the addition of RETA, the residual amount of RETA-PVA after complete combustion has been greatly increased, which is 30 times higher than that of PVA. The reason may be due to the inherent rigid structure of RE and the high carbon content of TA that cause the RETA to have higher carbon forming properties than TA-PVA. More residual carbon suggests that the formed expanded carbon layer delays the heat and flame propagation on the substrate surface during the combustion process.

The cone calorimeter test indicates that the addition of RETA can improve the flame retardancy of TA-PVA. When the ratio of RE : TA is 3 : 7, the heat release rate of the prepared RETA-PVA is significantly decreased, and the smoke production rate is also decreased significantly, and the carbon residue increases significantly, but there is still a slight increase in total heat release compared to RE-PVA and TA-PVA.

3.4 Morphology analysis of residual carbon of RE-PVA/TA-PVA/RETA-PVA

The study on char residue after complete combustion is one of the key factors to explore the flame retardant mechanism of RE/TA.[32] PVA almost had no carbon residue left after combustion.

Table 4 Cone test data of PVA/RE-PVA/TA-PVA/RETA-PVA

Sample	TTI (s)	Peak-HRR (kW m^{-2})	THR (MJ m^{-2})	Peak-SPR (m^2 s^{-1})	MLR (g s^{-1})	Mass retention (wt%)
PVA	61	634.9	58.5	0.180	0.30	0.3
TA-PVA	94	488.2	40.2	0.159	0.32	0.3
RE-PVA	74	273.9	25.3	0.084	0.16	12.5
RETA-PVA-1	83	398.1	43.7	0.127	0.27	8.7
RETA-PVA-2	84	399.1	40.5	0.101	0.26	9.3
RETA-PVA-3	77	391.1	45.2	0.118	0.25	9.2
RETA-PVA-4	78	419.7	42.5	0.101	0.26	8.5

The digital photos of char residue morphology for RE-PVA/TA-PVA/RETA-PVA are shown in Fig. 8. As shown in Fig. 8(a), the amount of residual carbon was insufficient and the formed carbon layer surface was loose and discontinuous after complete combustion of TA-PVA. After the addition of RE, the amount of residual carbon increased greatly, and the prepared four samples with RETA all formed a relatively complete carbon layer. It is ascribed to the addition of RE that can promote the formation of carbon. RETA-PVA expands and produces gas when it burns, forming an expanded carbon layer that protects the PVA matrix. It can be seen from the residual carbon photos of RETA-PVA that the formed carbon layer is relatively dense and only a few holes and cracks after RETA-PVA-3 combustion. After RETA-PVA-4 combustion, the formed carbon layer displays obvious cracks and a large number of holes. It means that RETA can promote char-formation of the PVA matrix. However, the carbon residue does not increase with the increase of RE. When the ratio of RE : TA is 3 : 7, the residual carbon is the densest.

In order to further investigate the flame retardant mechanism of RETA, the microstructure of residual carbon after cone test of TA-PVA, RE-PVA and RETA-PVA was assessed by SEM, as shown in Fig. 9. TA-PVA has a small amount of residual carbon and the formed carbon layer is discontinuous after cone test. It can be observed from Fig. 9(a) that there are a large number of holes and uneven pits on the surface of TA-PVA, which may be due to the insufficient char-formation of TA during combustion, resulting in the carbon layer cannot effectively protect the matrix and the main chain of PVA is broken. As shown in Fig. 9(b), there are also many holes on the surface of RE-PVA. Fig. 9(c–f) shows the microstructure of the residual carbon of RETA-PVA. Compared with Fig. 9(a) and (b), it can be observed that the addition of RETA can significantly improve the charring effect of samples, and the surface of the RETA-PVA carbon layer

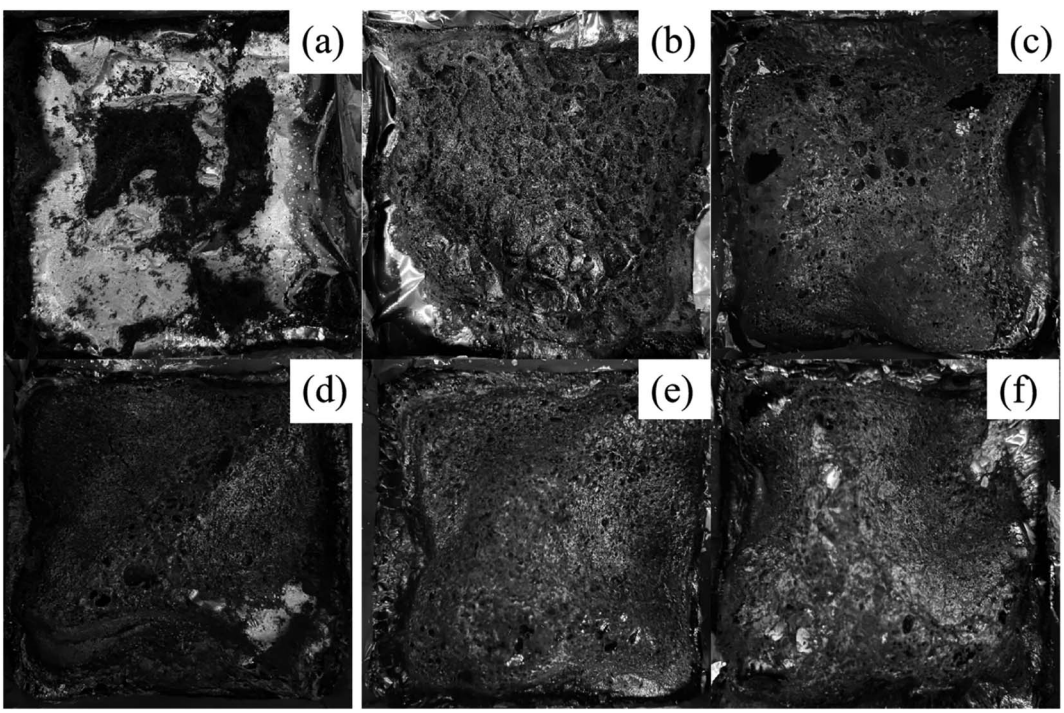

Fig. 8 Digital photos of carbon residues in TA-PVA/RE-PVA/RETA-PVA blends: (a) TA-PVA, (b) RE-PVA, (c) RETA-PVA-1, (d) RETA-PVA-2, (e) RETA-PVA-3, (f) RETA-PVA-4.

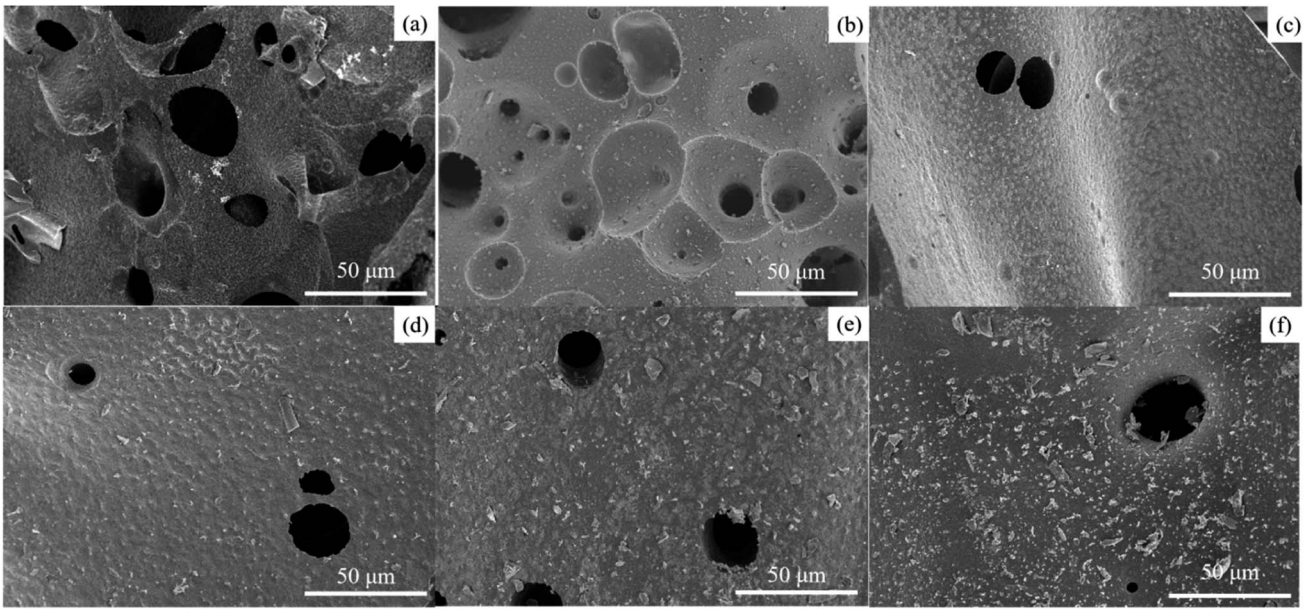

Fig. 9 SEM images of carbon residues in TA-PVA/RE-PVA/RETA-PVA blends: (a) TA-PVA, (b) RE-PVA, (c) RETA-PVA-1, (d) RETA-PVA-2, (e) RETA-PVA-3, (f) RETA-PVA-4.

is flat and there are only a few holes. Moreover, it can be observed that the amount of coated residual carbon on the sample surface is also increased with the increase of RE content in RETA-PVA. The coated residual carbon can effectively reduce the heat transfer among the matrix during combustion. At the same time, the complete and continuous carbon layer can prevent the release of heat and flue gas, inhibit the heat transfer among the matrix and effectively protect the matrix from rapid decomposition, which plays a role of condensed phase flame retardancy. Therefore, the addition of RETA can effectively promote the carbonization of the matrix, forms a more continuous and complete carbon layer, improves the flame retardancy of blends.

3.5 Mechanical properties of PVA and RE-PVA/TA-PVA/RETA-PVA blends

The flexural strength and impact strength of PVA and RE-PVA/TA-PVA/RETA-PVA blends are shown in Fig. 10(a) and (b), respectively. It can be seen form Fig. 10 that RE-PVA exhibits the worst mechanical properties, indicating that the addition of RE alone leads to a great effect on the mechanical properties of the matrix. As can be seen, the flexural strength and impact strength of the blends also decreased after adding RETA. The flexural strength decreased from 75.9 MPa to 36.6 MPa and the impact strength decreased from 8.7 kJ m^{-2} to 6.0 kJ m^{-2}. It may be due to the fact that the low hydrogen bond density between RETA and PVA, resulting in the reduction of the flexural and impact strength of RE-PVA. However, the flexural strength and impact strength of RETA-PVA had been improved with the difference of TA/RE ratio in RETA-PVA, which may be due to the fact that the number of hydrogen bonds between RETA and PVA increases with the increase of RE/TA ratio, and the increase of hydrogen bond density between RETA and PVA leads to the improvement of flexural strength and impact strength of RETA-PVA. It can be seen from Fig. 10 that the flexural strength of RETA-PVA-4 increased from 36.6 MPa to 49.3 MPa, which is 34.7% higher than that of RETA-PVA-1, and the impact strength increased from 6.0 kJ m^{-2} to 6.7 kJ m^{-2}.

4 Conclusion

In this paper, the effects of different TA/RE ratios on the flame retardancy of RETA-PVA blends have been studied. The stable hydrogen bonding among RETA-PVA molecules was demonstrated by Fourier transform infrared spectroscopy. Thermogravimetric analysis results indicate that the residue carbon for RETA-PVA-1 is 25% at 600 °C, which is 316.7% higher than that for PVA. The maximum decomposition rate of RETA-PVA is lower than that of PVA, indicating that RETA-PVA has relatively better thermal stability. DSC results indicate that RETA-PVA is amorphous and it has higher glass transition temperature than that of TA-PVA and RE-PVA. The glass transition temperature of RETA-PVA-2 is 51.3 °C, which is the highest among all blends. The cone calorimeter test results demonstrate that the peak-HRR decreases from 634.9 kW m^{-2} of PVA to 391.1 kW m^{-2} of RETA-PVA-3. The smoke production rate for RETA-PVA-2 is 43.9% lower than that for PVA, and the residual amount of RETA-PVA-2 is 30 times higher that of PVA after complete combustion. Comparing the residual carbon digital photos and SEM images of PVA, RE-PVA, TA-PVA and RETA-PVA, it can be observed that RETA-PVA forms a continuous and relatively complete carbon layer after complete combustion with the

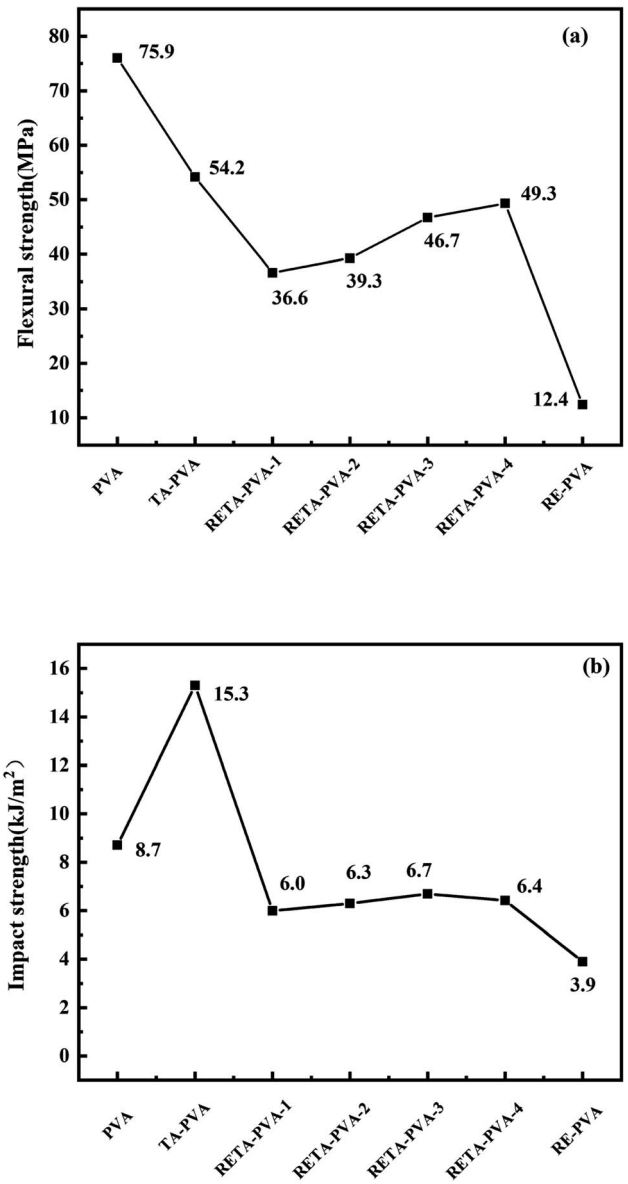

Fig. 10 Flexural strength (a) and impact strength (b) of PVA and TA-PVA/RE-PVA/RETA-PVA blends.

addition of RETA. RETA plays a role of condensed phase flame retardancy.

Availability of data and materials

All data needed to evaluate the conclusions in the paper are present in the paper. Additional data related to this paper may be requested from the corresponding author.

Author contributions

Yuan Lin: methodology, validation, formal analysis, resources, data curation, writing – original draft. Jialian Chen: investigation. Hongzhou Li: conceptualization, writing – review & editing, supervision, project administration, funding acquisition.

Conflicts of interest

The authors declare that they have no known competing financial interests or personal relationships that could have appeared to influence the work reported in this paper.

Acknowledgements

This work was supported by the Startup Fund from Fujian Normal University and the Natural Science Foundation of Fujian Province of China (2021J01198).

References

1 M. Korey, A. Johnson, W. Webb, M. Dietenberger, J. Youngblood and J. Howarter, Tannic acid-based prepolymer systems for enhanced intumescence in epoxy thermosets, *Green Mater.*, 2020, **8**, 150–161.
2 L. Costes, F. Laoutid, S. Brohez and P. Dubois, Bio-based flame retardants: when nature meets fire protection, *Mater. Sci. Eng., R*, 2017, **117**, 1–25.
3 W. Zhang, Z. Yang, R. Tang, J. Guan and Y. Qiao, Application of tannic acid and ferrous ion complex as eco-friendly flame retardant and antibacterial agents for silk, *J. Cleaner Prod.*, 2020, **250**, 119545.
4 Y. G. Daniel and B. A. Howell, Phosphorus flame retardants from isosorbide bis-acrylate, *Polym. Degrad. Stab.*, 2018, **156**, 14–21.
5 L. Ai, S. Chen, J. Zeng, P. Liu, W. Liu, Y. Pan and D. Liu, Synthesis and flame retardant properties of cyclophosphazene derivatives containing boron, *Polym. Degrad. Stab.*, 2018, **155**, 250–261.
6 Q. Wang, J. Guo, D. Xu, J. Cai, Y. Qiu, J. Ren and L. Zhang, Facile construction of cellulose/montmorillonite nanocomposite biobased plastics with flame retardant and gas barrier properties, *Cellulose*, 2015, **22**(6), 3799–3810.
7 Z. Xia, W. Kiratitanavit, P. Facendola, S. Yu, J. Kumar, R. Mosurkal and R. Nagarajan, A bio-derived char forming flame retardant additive for nylon 6 based on crosslinked tannic acid, *Thermochim. Acta*, 2020, **693**, 178750.
8 L. Xu, K.-G. Neoh and E. Kang, Natural polyphenols as versatile platforms for material engineering and surface functionalization, *Prog. Polym. Sci.*, 2018, **87**, 165–196.
9 B. A. Howell and X. Han, Effective biobased phosphorus flame retardants from starch-derived bis-2,5-(hydroxymethyl) furan, *Molecules*, 2020, **25**(3), 592.
10 R. A. Gross and B. Kalra, Biodegradable Polymers for the Environment, *Science*, 2002, **297**(5582), 803–807.
11 K. Hwa Hong, Preparation and properties of polyvinyl alcohol/tannic acid composite film for topical treatment application, *Fibers Polym.*, 2016, **17**, 1963–1968.
12 X. Jin, E. Xiang, R. Zhang, D. Qin, M. Jiang and Z. Jiang, Halloysite nanotubes immobilized by chitosan/tannic acid complex as a green flame retardant for bamboo fiber/poly (lactic acid) composites, *J. Appl. Polym. Sci.*, 2020, **138**, 49621.
13 T. S. Sileika, D. G. Barrett, R. Zhang, K. H. Aaron Lau and P. B. Messersmith, Colorless multifunctional coatings

inspired by polyphenols found in tea, chocolate, and wine, *Angew. Chem., Int. Ed.*, 2013, **52**, 10766–10770.
14 F. Reitzer, M. Allais, V. Ball and F. Meyer, Polyphenols at interfaces, *Adv. Colloid Interface Sci.*, 2018, **257**, 31–41.
15 Y.-O. Kim, J. Cho, Y. N. Kim, K. W. Kim, B. W. Lee, J. W. Kim, M. Kim and Y. C. Jung, Recyclable, flame-retardant and smoke-suppressing tannic acid-based carbon-fiber-reinforced plastic, *Composites, Part B*, 2020, **197**, 108173.
16 Y.-O. Kim, J. Cho, H. Yeo, B. W. Lee, B. J. Moon, Y. Ha, Y. R. Jo and Y. C. Jung, Flame retardant epoxy derived from tannic acid as biobased hardener, *ACS Sustainable Chem. Eng.*, 2019, **7**, 3858–3865.
17 H. Peng, D. Wang and S. Fu, Tannic acid-assisted green exfoliation and functionalization of MoS_2 nanosheets: significantly improve the mechanical and flame-retardant properties of polyacrylonitrile composite fibers, *Chem. Eng. J.*, 2020, **384**, 123288.
18 W. Wang, Q. Tang, T. Yu, X. Li, Y. Gao, J. Li, Y. Liu, L. Rong, Z. Wang, H. Sun, H. Zhang and B. Yang, Surfactant-free preparation of Au@resveratrol hollow nano-particles with photothermal performance and antioxidant activity, *ACS Appl. Mater. Interfaces*, 2017, **9**, 3376–3387.
19 Z. Marion, D. Micheline, B. Jean-Luc, P. Christine and C. Gregory, Trans-resveratrol and trans-ε-viniferin in grape canes and stocks originating from Savoie Mont Blanc vineyard region: pre-extraction parameters for improved recovery, *ACS Sustainable Chem. Eng.*, 2019, **7**, 8310–8316.
20 Y. Tian, Q. Wang, K. Wang, M. Ke, Y. Hu, L. Shen, Q. Geng, J. Cheng and J. Zhang, From biomass resources to functional materials: a fluorescent thermosetting material based on resveratrol via thiolene click chemistry, *Eur. Polym. J.*, 2019, **123**, 109416.
21 Z. Ulakcsai, F. Bagamery, E. Szoko and T. Tabi, The role of autophagy induction in the mechanism of cytoprotective effect of resveratrol, *Eur. J. Pharm. Sci.*, 2018, **123**, 135–142.
22 A. Mattarei, M. Azzolini, M. Carraro, N. Sassi, M. Zoratti, C. Paradisi and L. Biasutto, Acetal derivatives as prodrugs of resveratrol, *Mol. Pharm.*, 2013, **10**(7), 2781–2792.
23 L. Huminiecki and J. Horbanczuk, The functional genomic studies of resveratrol in respect to its anti-cancer effects, *Biotechnol. Adv.*, 2018, **36**(6), 1699–1708.
24 J. J. Cash, M. C. Davis, M. D. Ford, T. J. Groshens, A. J. Guenthner, B. G. Harvey, K. R. Lamison, J. M. Mabry, H. A. Meylemans, J. T. Reams and C. M. Sahagun, High Tg thermosetting resins from resveratrol, *Polym. Photochem.*, 2013, **4**, 3859–3865.
25 K. Zhang, M. Han, L. Han and H. Ishida, Resveratrol-based tri-functional benzoxazines: synthesis, characterization, polymerization, and thermal and flame retardant properties, *Eur. Polym. J.*, 2019, **116**, 526–533.
26 Y. Tian, Q. Wang, L. Shen, Z. Cui, L. Kou, C. Jue and J. Zhang, A renewable resveratrol-based epoxy resin with high Tg, excellent mechanical properties and low flammability, *Chem. Eng. J.*, 2019, **383**, 123124.
27 W. Niu, Y. Zhu, R. Wang, Z. Lu, X. Liu and J. Sun, Remalleable, healable, and highly sustainable supramolecular polymeric materials combining superhigh strength and ultrahigh toughness, *ACS Appl. Mater. Interfaces*, 2020, **12**, 30805–30841.
28 H. Ejima, J. J. Richardson, K. Liang, J. P. Best, M. P. van Koeverden, G. K. Such, J. Cui and F. Caruso, One-step assembly of coordination complexes for versatile film and particle engineering, *Science*, 2013, **341**, 154–157.
29 D. Lee, H. Hwang, J.-S. Kim, J. Park, D. Youn, D. Kim, J. Hahn, M. Seo and H. Lee, Vata: poly (vinyl alcohol)- and tannic acid-based nontoxic underwater adhesive, *ACS Appl. Mater. Interfaces*, 2020, **12**, 20933–20941.
30 J. Zheng, B. Li, C. Guo, Q. Wu and Y. Wang, Flame-retardant properties of acrylonitrile-butadiene-styrene/wood flour composites filled with expandable graphite and ammonium polyphosphate, *J. Appl. Polym. Sci.*, 2014, **131**(10), 376–418.
31 W. Xie, Q. Bao, Y. Liu, H. Wen and Q. Wang, Hydrogen bond association to prepare flame retardant polyvinyl alcohol film with high performance, *ACS Appl. Mater. Interfaces*, 2021, **13**(4), 5508–5517.
32 D. Yang, L. Dong, X. Hou, W. Zheng, J. Xiao, J. Xu and H. Ma, Synthesis of bio-based poly (cyclotriphosphazene-resveratrol) microspheres acting as both flame retardant and reinforcing agent to epoxy resin, *Polym. Adv. Technol.*, 2019, **31**(1), 135–145.